Surface chemistry of amphiphilic polysiloxane/triethyleneglycol-modified poly(pentafluorostyrene) block copolymer films before and after water immersion

Elisa Martinelli[a*], Gabriele Pelusio[a], Bhaskar R. Yasani[a], Antonella Glisenti[b], Giancarlo Galli[a]

[a]*Dipartimento di Chimica e Chimica Industriale and UdR Pisa INSTM, Università di Pisa, 56124 Pisa, Italy;* [b]*Dipartimento di Scienze Chimiche, Università di Padova, 35131 Padova, Italy*

New amphiphilic block copolymers Si-EFS*x* composed of a poly(dimethyl siloxane) (Si) block and a poly(4-(triethyleneglycol monomethyl ether)-2,3,5,6-tetrafluorostyrene) (EFS) block were synthesized by ATRP starting from a bromo-terminated Si macroinitiator. Similarly, new hydrophobic block copolymers Si-FS*y* consisting of an Si block and a poly(pentafluorostyrene) (FS) block were prepared for comparison. X-ray photoelectron spectroscopy (XPS) analysis on block copolymer films revealed that the Si block was concentrated at the polymer–air interface, while the EFS block was located in the layers underneath. The same polymer films underwent a marked surface reconstruction after immersion in water for seven days, as probed by XPS. This phenomenon involved the exposure of the hydrophilic oxyethylenic chains to contact

water. Such surface reconstruction was even more drastic when an amphiphilic block copolymer was dispersed in a cross-linked poly(dimethyl siloxane) matrix film.

Keywords: poly(pentafluorostyrene), block copolymer, surface reconstruction, amphiphilic copolymer, XPS

1. Introduction

Amphiphilic block copolymers are a special class of materials with hydrophilic and hydrophobic components, capable of forming self-assembled nanostructures either in solution[1] or in the solid state.[2] Their phase-separated domains can be selectively endowed with specific chemical functionalities and using the self-organization aspects of structure formation and the different interactions with the external environment the functions can be changed under the influence of external stimuli such as contact liquids, temperature, pH or ionic strength.[3–6] Recently, amphiphilic block copolymers have been evaluated for biomedical applications[7–9] and as environmentally friendly coatings to prevent marine biofouling.[10,11] In this research area, several amphiphilic block copolymer structures are reported in the literature consisting of perfluoroalkyl and poly(ethylene glycol) (PEG) chains that are located in either separate blocks[12,13] or in the same block as mixed grafted ethoxylated-fluoroalkyl side chains.[14–16] We are interested in developing amphiphilic polymer films in which the hydrophilic/hydrophobic balance character of the surface is varied by reorganization of the surface chemical composition after exposure to water.[15,17] This reconstruction may be exploited to direct/reduce several interfacial processes such as cell proliferation, protein adsorption

and fouling adhesion.[18] Specifically, the dynamical surface chemical changes over different time scales of contact with water have been reported to prevent strong adhesion and to facilitate release of marine biofouling organisms.[19]

In the present work, we investigated novel amphipilic diblock copolymers composed of a poly(dimethylsiloxane) (Si) first block and a modified pentafluorostyrene second block carrying a triethyleneglycol monomethyl ether chain in *para* position. Such a block is expected to display an amphiphilic behaviour, in that the hydrophilic and hydrophobic constituents are incorporated into one same polymer component. In fact, fluorinated polymers are known for their low wetting properties, being simultaneously hydrophobic and lipophobic.[20] On the other hand, PEG is a water soluble polymer which has a high surface energy and a low interfacial energy with water.[21] Thus, upon contact of the copolymer film with water a reconstruction might be anticipated to involve the exposure of the oxyethylenic side chains to maximize their contact with water as dragged close to the film surface by the perfluorinated aromatic rings carrying them. Moreover, the polysiloxane block was chosen to compatibilize the block copolymers with a PDMS matrix to obtain low-elastic modulus amphiphilic blend networks, possibly applicable as marine fouling resistant coatings.[22] We used the X-ray photoelectron spectroscopy (XPS) to probe the surface chemical structure of the polymer films and to confirm its reconstruction response to contact with water.

2. Experimental Section

2.1. Materials

Tetrahydrofuran (THF), anisole and triethylamine were distilled under nitrogen prior to use. Monocarbinol-terminated polydimethyl siloxane (Si-OH, M_n = 1000 g mol^{-1}, M_w/M_n ~ 1.2) (Gelest), bis(silanol)-terminated poly(dimethyl siloxane) (HO-PDMS-OH) (M_n = 26,000 g mol^{-1}), poly(diethoxy siloxane) (ES40) (M_n = 134 g mol^{-1}), 2,3,4,5,6-pentafluorostyrene (FS, Aldrich 99%), triethyleneglycol monomethyl ether (TEG, Aldrich 95%), bismuth neodecanoate (BiND, Sigma-Aldrich), 2-bromo-isobutyryl bromide (BIBB, Aldrich 98%), CuBr (Aldrich 99.9%) and 2,2'-bipyridyl (bipy, Aldrich ≥ 99%) were used without further purification.

2.2. Monomer 4-(triethyleneglycol monomethyl ether)-2,3,5,6-tetrafluorostyrene (EFS) and macroinitiator Si-Br

EFS and Si-Br were synthesized by modifications of literature procedures in ref.[23] and ref.[24], respectively. Experimental details are given in the Supporting Information.

2.3. Synthesis of block copolymers Si-EFS*x*

In a typical copolymerization, 0.304 g (0.26 mmol) of Si-Br, 1.228 g (3.79 mmol) of EFS, 110 mg (0.70 mmol) of bipy and 5 mL of anisole were introduced into a dry Schlenk flask. After four freeze-thaw pump cycles, 38 mg (0.27 mmol) of CuBr was added under nitrogen and the solution was deoxygenated by three further freeze-thaw pump cycles. The polymerization was let to proceed under nitrogen for 64 h at 110 °C. When the reaction was stopped the polymer mixture was dissolved in chloroform and passed through a neutral alumina column. The solvent was removed under vacuum and the polymer was purified by repeated extractions with *n*-hexane (46% yield). The

resulting block copolymer, with average degree of polymerization *x* of the EFS block equal to 14, is denoted by Si-EFS14.

^{1}H NMR ($CDCl_3$): δ (ppm) = 0.1 ($SiCH_3$), 0.5 ($SiCH_2$), 0.9 ($CH_2C\underline{H}_3$), 1.3 ($C\underline{H}_2CH_2Si$), 1.6 ($CH_3C\underline{H}_2$), 1.9 (CCH_3), 1.9–2.9 ($C\underline{H}_2C\underline{H}Ph$), 3.3 ($OCH_3$), 3.5–3.9 ($CH_2O$, $COOCH_2C\underline{H}_2OC\underline{H}_2$), 4.4 ($COOCH_2$, $PhOCH_2$).

^{19}F NMR ($CDCl_3$/CF_3COOH): δ (ppm) = –82 (*m*-F), –68 (*o*-F).

2.4. Synthesis of block copolymers Si-FS*y*

In a typical copolymerization, 0.426 g (0.37 mmol) of Si-Br, 1.108 g (5.71 mmol) of FS, 180 mg (1.10 mmol) of bipy and 5 mL of anisole were introduced into a dry Schlenk flask. After four freeze-thaw pump cycles, 43 mg (0.30 mmol) of CuBr was added under nitrogen and the solution was deoxygenated by three further freeze-thaw pump cycles. The polymerization was let to proceed under nitrogen for 64 h at 110 °C. When the reaction was stopped the polymer mixture was dissolved in chloroform and passed through a neutral alumina column. The solvent was removed under vacuum and the polymer was purified by repeated precipitations into methanol (57% yield). The resulting block copolymer, with average degree of polymerization *y* of the FS block equal to 19, is denoted by Si-FS19.

^{1}H NMR ($CDCl_3$): δ (ppm) = 0.1 ($SiCH_3$), 0.5 ($SiCH_2$), 0.9 ($CH_2C\underline{H}_3$), 1.3 ($C\underline{H}_2CH_2Si$), 1.6 ($CH_3C\underline{H}_2$), 1.9 (CCH_3), 1.9–2.9 ($C\underline{H}_2C\underline{H}Ph$), 3.5 ($COOCH_2CH_2OC\underline{H}_2$), 3.7 ($COOCH_2C\underline{H}_2O$), 4.4 ($COOCH_2$).

^{19}F NMR ($CDCl_3$/CF_3COOH): δ (ppm) = –85 (*m*-F), –78 (*p*-F), –68 (*o*-F).

2.5. Preparation of PDMS-blends and copolymer films

Squared (18 × 18 mm^2) glass slides were cleaned with acetone and dried in oven for 30 min.

Polymer films were prepared by spin coating a 3% (w/w) $CHCl_3$ solution of each polymer on glass slides (thickness ~ 300 nm).

PDMS-blend films were prepared by spin coating a solution of HO-PDMS-OH (5.0 g), ES40 (0.125 g), BiND (50 mg), block copolymer Si-EFS71 (400 mg) and ethyl acetate (25 mL) on glass slides (thickness ~ 500 nm). Therefore, the block copolymer was physically dispersed, not chemically linked, within the PDMS matrix in a semi-interpenetrating cross-linked network. The blend containing 8 wt% block copolymer with respect to the PDMS matrix is denoted as Si-EFS71_8.

In any case, the films after coating were kept at room temperature for 12 h and then at 120 °C for 12 h. At this temperature the block copolymer migration to the surface was also facilitated.

2.6. Characterization

^{1}H NMR (*vs* $CDCl_3$) and ^{19}F NMR (*vs* CF_3COOH) spectra were recorded with a Varian Gemini VRX300 spectrometer. The number and weight average molecular weights of the polymers (M_n and M_w) were determined by size exclusion chromatography (SEC) with a Jasco PU-1580 liquid chromatograph equipped with two PL gel 5 μm Mixed-D columns and a Jasco 830-RI refractive index detector. Polystyrene standards (from 400 g mol^{-1} to 400000 g mol^{-1}) were used for calibration.

Differential scanning calorimetry (DSC) analysis was performed with a Mettler DSC-30 instrument from –160 to 100 °C at heating/cooling rate of 10 °C min^{-1} under a dry nitrogen flow. The glass transition temperature (T_g) was taken as the inflection temperature in the second heating cycle and the associated heat capacity change (ΔC_p) was evaluated with indium calibration.

Contact angles with water and *n*-hexadecane (θ_w and θ_h) were measured on films before immersion in water using the sessile drop method with a Camtel FTA200 goniometer at room temperature. They were then used to determine the surface free energy (γ_S) of the polymer films using the Owens–Wendt–Kaelble method.[25,26]

X-ray photoelectron spectroscopy (XPS) spectra were recorded by using a Perkin-Elmer PHI 5600 spectrometer with a standard Al–Kα source (1486.6 eV) operating at 350 W. The working pressure was less than 10^{-8} Pa. The spectrometer was calibrated by assuming the binding energy (BE) of the Au $4f_{7/2}$ line to be 84.0 eV with respect to the Fermi level). Extended (survey) spectra were collected in the range 0–1350 eV (187.85 eV pass energy, 0.4 eV step, 0.05 s $step^{-1}$). Detailed spectra were recorded for the following regions: C(1s), O(1s), F(1s) and Si(2p) (11.75 eV pass energy, 0.1 eV step, 0.1 eV s $step^{-1}$). The standard deviation in the BE values of the XPS line was 0.10 eV. The spectra were recorded at two photoemission angles ϕ (between the surface normal and the path taken by the photoelectrons) of 70° and 20°, corresponding to sampling depths of ~ 3 nm and ~ 10, respectively. The atomic percentage, after a Shirley type background subtraction,[27] was evaluated using the PHI sensitivity factors (±1% experimental error).[28] To take into account charging problems, the C(1s) peak was considered at 285.0 eV and the peak BE differences were evaluated. The XPS peak fitting procedure was

carried out, after a Shirley type background subtraction, by means of Voigt functions and the results were evaluated through the χ^2 function.[29]

3. Results and Discussion

3.1. Synthesis

The block copolymers were synthesized in a two-step procedure (Figure 1). Firstly, a bromo-terminated PDMS macroinitiator Si-Br was prepared.[24,30] The average molecular weight of the Si-Br was ~ 1200 g mol^{-1} (average polymerization degree of 11) with a polydispersity of ~ 1.2. Secondly, the prepared macroinitiator was used for the ATRP of 2,3,4,5,6-pentafluorostyrene (FS) and 4-(triethyleneglycol monomethyl ether)-2,3,5,6-tetrafluorostyrene (EFS) monomers. The ATRP of both FS and EFS was carried out at 110 °C for 64 h using CuBr as catalyst, 2,2'-bipyridyl (bipy) as ligand and anisole as solvent. ATRP is, in fact, a versatile method for the controlled radical polymerization of FS and other monomers derived from FS.[31] The resulting block copolymers are denoted as Si-EFS*x* and Si-FS*y*, where *x* and *y* indicate the polymerization degrees of the fluorinated blocks (Table 1). The formation of block copolymer structures with attachment of the fluorinated block was confirmed by ^{19}F NMR spectroscopy investigations. The chemical composition of the copolymers was evaluated from the integrated areas of the ^{1}H NMR signals at 0.0 ppm ($Si(CH_3)_2$ of Si block) and 2.4–3.0 ppm (CH_2, CH of the main chain of FS block) or 4.4 ppm (OCH_2 of EFS). In both Si-EFS*x* and Si-FS*y* block copolymers, the Si block length was constant while the length, and consequently the molar percentage, of the EFS and FS blocks was increased by

increasing the monomer/Si-Br macroinitiator feed mole ratio. Owing to the ATRP, the lengths of the fluorinated second block were tailored to be similar, so that Si-FS*y* copolymers were used as model copolymers to compare with the novel amphiphilic Si-EFS*x* block copolymers. All the polymers exhibited a monomodal distribution up to relatively high conversions (Figure 2) with a relatively narrow molecular weight polydispersity (M_w/M_n = 1.1–1.2) (Table 1). The values of the molecular weight evaluated by SEC were generally lower than those obtained by NMR. This difference results from the fact that the former technique provides approximate values of M_n as the block copolymers have different hydrodynamic volumes from those of the polystyrene standards used for calibration.

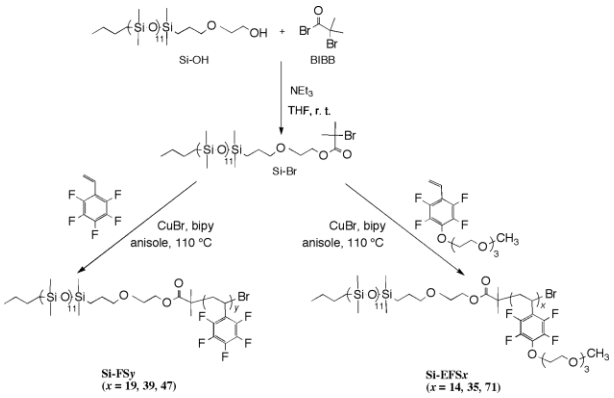

Figure 1. Synthesis of ATRP diblock copolymers Si-EFS*x* and Si-FS*y*.

DSC analyses revealed that each class of block copolymers exhibited an amorphous thermal behaviour that depended on both chemistry and composition of the block copolymer (Table S1). Generally, the copolymers displayed two glass transitions. The lower temperature transition, in the range –108 °C to –130 °C, was attributed to the Si block, while the higher temperature transition was due to the EFS or FS block. This increased with the block length from 56 °C for y = 19 to 82 °C for y = 47 in copolymers

Si-FS*y* and was centered at ~ –55 °C, with no significant change with increased *x*, in copolymers Si-EFS*x*. In any case, the T_g values of the polymer blocks were correlated with those of the corresponding homopolymers (Table S1), indicating that the two blocks of the copolymers were poorly miscible and microphase separated in their amorphous phases.

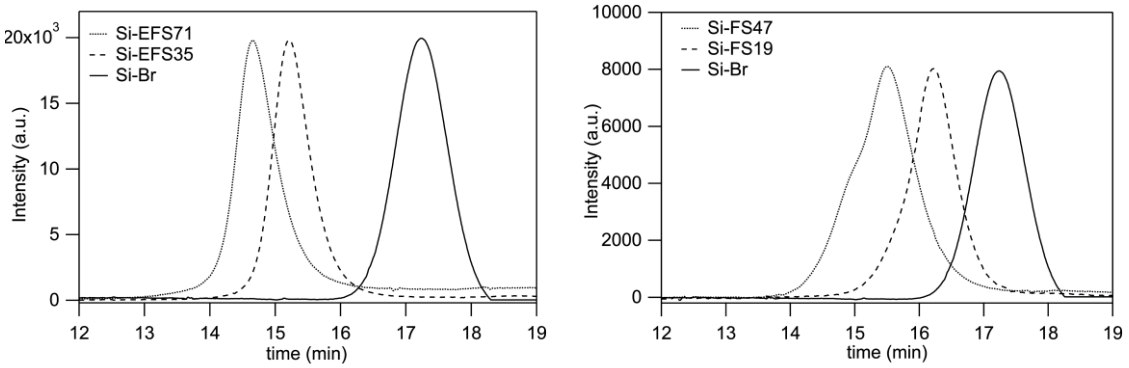

(a) (b)

Figure 2. SEC traces of macroinitiator Si-Br and the corresponding diblock copolymers (a) Si-EFS*x* and (b) Si-FS*y*.

3.2. Contact angles and surface free energy of films

The static contact angles were measured for all the polymer films with both water (θ_w) and *n*-hexadecane (θ_h) (Table 2). Si-FS*y* block copolymers exhibited relatively high contact angles with water (θ_w ~ 100°), but not as high as expected of highly hydrophobic polystyrenes or poly(acrylate)s carrying dangling fluorinated chains.[32–34] Moreover, they showed low values of θ_h, indicating the poor lipophobic character of the polymer surface. However, both θ_w and θ_h were significantly higher than those of the siloxane

macroinitiator, suggesting that the pentafluorostyrene block was segregated at the surface and contributed to decrease the wettability. On the other hand, Si-EFS*x* block copolymers showed θ_h and θ_w values comparable to and lower than those of the corresponding Si-FS*y* copolymers, essentially independent of the length of the EFS block.

From θ_w and θ_h measurements, the values of surface free energy γ_S were calculated by the additive component method of Owens–Wendt–Kaelble (Table 2).[25,26] Copolymers Si-FS*y* showed relatively high surface free energy values (γ_S = 23.9–24.7 mN m^{-1}) as a consequence of their weak lipophobic behaviour. For copolymers Si-EFS*x* the calculated γ_S was higher (γ_S = 27.3–27.8 mN m^{-1}) because of their comparatively low hydrophobicity. In any case, the dispersion component of γ_S was predominant (γ_S^d ~ 23.6–23.8 mN m^{-1}) owing to the preferred apolar interactions. The polar component was minimal for copolymers Si-FS*x* (γ_S^p ~ 0.6–1.3 mN m^{-1}) and became more significant for copolymers Si-EFS*x* (γ_S^p ~ 3.7–4.0 mN m^{-1}) because of polar, e.g. hydrogen bonding, interactions. The lower values of θ_w and higher values of γ_S in general, and γ_S^p in particular, may be due to a poorer tendency of EFS block to migrate to the surface in comparison to the FS block. Moreover, the presence of the oxyethylenic chains can further decrease θ_w and increase γ_S.

To confirm the occurrence of these phenomena an XPS analysis was carried out on films of copolymers Si-EFS*x* and Si-FS*y* containing the highest and lowest amounts of fluorinated units. The former films were also investigated after immersion in water.

3.3. Surface chemical composition

The atomic surface percent composition of the copolymers Si-EFS14 and Si-EFS71 was

determined at the two photoemission angles ϕ of 70° and 20° by angle-resolved XPS measurements. The surface composition of (non-ethoxylated) block copolymers Si-FS19 and Si-FS47 and homopolymers P(EFS) and P(FS) were also evaluated for comparison. Experimental data are summarized in Table 3, where they are also compared with the theoretical values calculated from the known stoichiometry of the polymers.

For the former two block copolymers the fluorine concentration increased with the length of the fluorinated block, e.g. from 10% to 14% at ϕ = 20° in going from x = 14 to x = 71, value at which the F% was similar to that of the homopolymer P(EFS). The experimental F% was generally lower than the theoretical one and increased with sampling depth, e.g. from 4% to 10% in going from ϕ = 70° to ϕ = 20° for Si-EFS14. On the other hand, Si% was higher than the theoretical one and followed the opposite trend with ϕ. This is in contrast to what was observed for other siloxane/fluorinated copolymer films, where the fluorinated component was much more strongly surface segregated than the siloxane component, e.g. $F\%_{exp}/F\%_{theor}$ and $Si\%_{exp}/Si\%_{theor}$ ratios were ~3 and ~0.5, respectively.[35] These findings indicate that a competition exists in populating the film surface between the two low surface energy Si and EFS blocks which results in a preferential segregation of the Si component to the polymer–air interface. Similar remarks are also valid for the block copolymers Si-FS19 and Si-FS47, even though their F% at the surface was obviously much higher than for the block copolymers Si-EFS. A relatively weak tendency to surface segregation of *para* modified poly(pentafluorostyrene)s has already been reported.[36] It was shown that polymer films of poly(tetrafluostyrene) carrying $(CF_2)_nF$ (n = 2, 7) side chains presented an experimental surface F% significantly lower than the theoretical one.

In any case, the C(1s) peak of Si-EFS copolymers showed a complex shape due to the presence of at least three overlapping contributions from different C-moieties centered at ~ 285 eV ($SiCH_3$, CH, CH_2), ~ 287 eV (C(CF), CH_2O) and ~ 288 eV (CF) (Figure S1).[37] Figure 3 shows the area-normalized C(1s) spectra at the two ϕ for the block copolymers Si-EFS14 and Si-EFS71. Taking the former copolymer as an illustration (Figure 3a), two trends are clearly seen with decreasing ϕ: (i) the signals with contributions from the CH_2O and CF groups rose in intensity from 21% and 3% to 31% and 7%, respectively, and (ii) the signal with contribution from the $SiCH_3$ groups had a reduced intensity from 76% to 62%. Moreover, the integrated areas of the signals at ~ 287 eV and ~ 288 eV were significantly lower than the theoretical ones (53% and 23%). By contrast, the area of the peak at ~ 285 eV was higher than the theoretical value (76% *vs* 24%). Overall, these results confirm those discussed above on the atomic composition as a function of the sampling depth with varying ϕ.

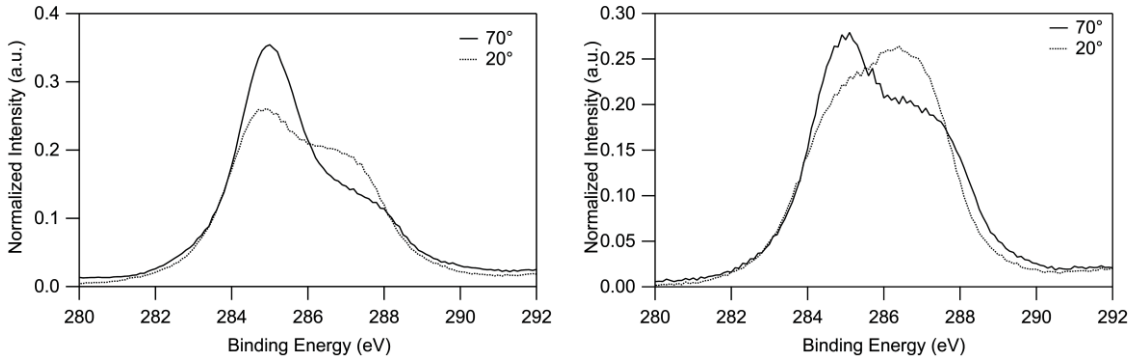

(a) (b)

Figure 3. Area-normalized C(1s) XPS signals at ϕ of 70° and 20° for the block copolymer films Si-EFS14 (a) and Si-EFS71 (b).

For copolymers Si-FS, the C(1s) contributions at ~ 285 eV ($SiCH_3$, CH, CH_2) and ~ 286 eV (C(CF)) on the one hand, and the contribution at ~ 288 eV (CF), on the other hand (Figure S2), were less and more intense, respectively, than the corresponding signals of Si-EFS copolymers (Figure 4a). However, the integrated areas of normalized signals at ~ 285 eV and ~ 288 eV followed the same trend with ϕ as previously discussed for copolymers Si-EFS (Figure 4b).

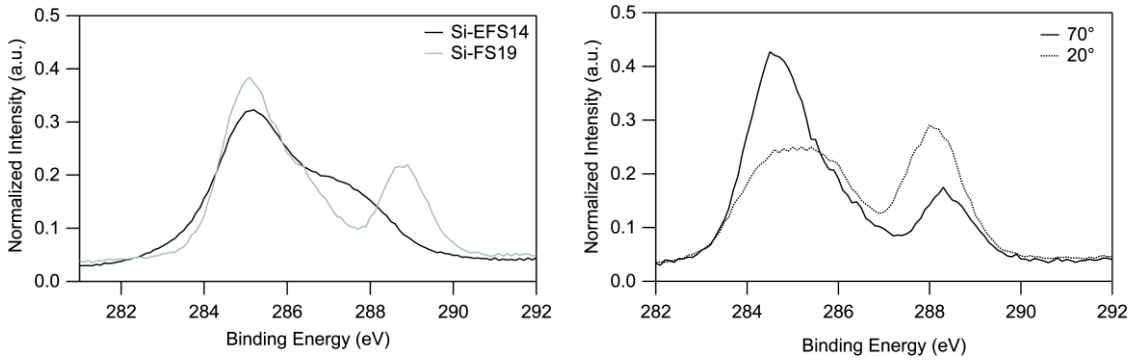

(a) (b)

Figure 4. Comparison of area-normalized C(1s) XPS signals of block copolymer films Si-EFS14 and Si-FS19 at ϕ of 70° (a) and area-normalized C(1s) XPS signals at ϕ of 70° and 20° for block copolymer film Si-FS47 (b).

The C(1s) XPS signal of Si-EFS71_8 blend at both ϕ consisted only of the contribution at ~ 285 eV, due to the $Si(CH_3)$ groups of the PDMS matrix, with the block copolymer being hidden in the deeper layers of the film surface (Figure 5).

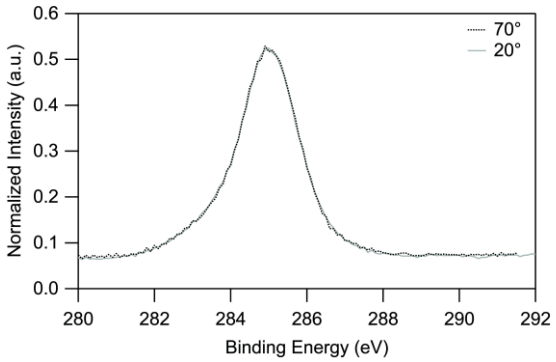

Figure 5. Area-normalized C(1s) XPS signals at photoemission angles of 70° and 20° for the blend film Si-EFS71_8.

An angle-resolved XPS analysis was also carried out on the amphiphilic Si-EFS copolymers after immersion in water for 7 days, with the aim of ascertaining whether the surface of the films could reorganize in response to the different outer environment. The surface composition of the films after immersion is expected to be that corresponding to a kinetically trapped condition, rather than the equilibrium state when in contact with water. The XPS spectra of the surface after immersion can, therefore, be considered indicative of the chemical composition when the surface is in contact with water. The atomic compositions of the surfaces after water immersion are also collected in Table 3. The elemental composition varied with ϕ and both Si% and F% followed the same trends discussed for the respective dry surfaces. The experimental composition of any polymer surface obtained at any given ϕ seemed not to change to a significant extent after immersion in water with respect to the dry surface. However, a close inspection of the C(1s) signal after water immersion enabled us to better understand the reconstruction processes occurred. In fact, the comparison of C(1s) signals before and after water immersion for a given sample and ϕ clearly shows that in any case the peaks due to CH_2O

and $Si(CH_3)$ groups increased and decreased, respectively, upon immersion in water (Figure 6). For example, for Si-EFS14 at $\phi = 20°$ the former increased from 31% to 38%, while the lstter decreased from 62% to 56%. On the other hand, the integrated area of the CF peak remained essentially unchanged before and after water immersion (7% and 6%, respectively), in agreement with the constant value of F%. Owing to the low surface energy of the fluorinated aromatic units, the oxyethylenic side chains are promptly placed in a region below the outer surface when the polymer is in contact with air. Consequently, they can readily expand outward after immersion in water to maximize their contact with water, in a sort of stretched conformation. Conversely, the methyl groups of the siloxane block, which populated the dry surfaces, move back into the bulk as a result of their hydrophobicity.

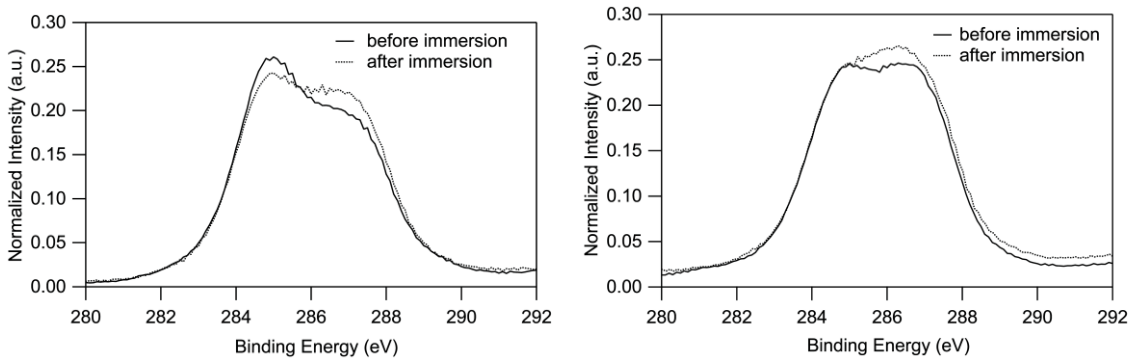

(a) (b)

Figure 6. Area-normalized C(1s) XPS signals at $\phi = 20°$ for the block copolymer films (a) Si-EFS14 and (b) Si-EFS71 before and after immersion in water for 7 days.

This reconstruction process was even more pronounced for the PDMS-blend Si-EFS71_8. In fact, the C(1s) peak of the film after immersion in water displayed a more complex shape than that of the dry film (Figure 7). In particular, the C(1s) signal was

composed of the same three contributions detected for the corresponding block copolymer Si-EFS71 (Figure S3). For the blend films both the integrated areas under the CH_2O (11%) and the CF (14%) peaks were markedly higher than the theoretical ones (7% and 3%, respectively), while that of the $Si(CH_3)$ was significantly lower (75% *vs* 90%). Evidently the EFS block was more strongly segregated from the PDMS matrix than the Si block. These findings indicate that the EFS block is hidden in the bulk when the blend is in contact with air, while the PDMS matrix covers the surface. However, the EFS block migrates to the outer surface layers (within ~ 10 nm from the polymer surface) after contact with water, being driven there by the enthalpically favourable polar interactions of the oxyethylenic chains with water.

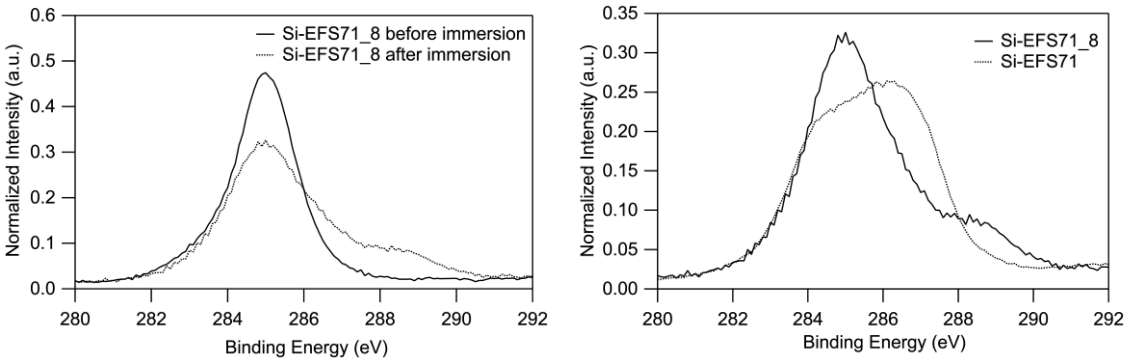

(a) (b)

Figure 7. Comparison of area-normalized C(1s) signals (ϕ = 20°) of films of (a) blend Si-EFS71_8 before and after water immersion and (b) blend Si-EFS71_8 and the corresponding block copolymer after water immersion.

4. Concluding Remarks

The new set of block copolymers Si-EFS have the unusual feature that both the

constituent blocks have low surface energy properties, which resulted in a competition to populate the outer surface of the film. In the dry state the Si block was preferentially segregated at the outermost surface, with the EFS component being mostly confined in the layers underneath. Comparison with the films of the hydrophobic Si-FS block copolymers confirmed that the Si block possessed a greater drive to surface segregate than the FS and EFS blocks. However, after contact with water the film surface reconstructed by exposing the oxyethylenic chains at the polymer–water. The surface reorganization of the immersed films was even more pronounced for the PDMS-blend films. In fact, while their dry surface was completely covered by a PDMS matrix layer, the surface after immersion in water became much richer in the EFS block of the copolymer. Therefore, these films are able to reduce their free interfacial energy by delivering energetically favorable segments to the polymer-surrounding environment interface and withdrawing unfavorable segments backwards at the same time. The capability of the block copolymers of this work to respond to the external environment, especially when embedded in a PDMS network, can be exploited to prepare atoxic, nonbiocidal coatings for marine applications in which the dynamical changes of a (nano)heterogeneous chemical surface can deter settlement and adhesion of fouling organisms.[18,38] The antifouling/fouling release properties of such coatings will be the subject of a future publication.

Supporting Information

Supporting Information is available from the Wiley Online Library or from the author.

Acknowledgments: Work supported by the Italian MiUR (PRIN fondi 2010-2011).

[1] A. Blanazs, S. P. Armes, A. J. Ryan, *Macromol. Rapid Commun*. **2009**, *30*, 267–277.

[2] L. Guo, Y. Jiang, S. Chen, T. Qiu, X. Li, *Macromolecules* **2014**, *47*,165–174.

[3] J. Rodríguez-Hernández, F. Checot, Y. Gnanou, S. Lecommandoux, *Prog. Polym. Sci.* **2005**, *30*, 691–724.

[4] A. K. Bajpai, S. K. Shukla, S. Bhanu, S. Kankane, *Prog. Polym. Sci.* **2008**, *33*, 1088–1118.

[5] E. Smith, X. Xu, C. L. McCormick, *Prog. Polym. Sci.* **2010**, *35*, 45–93.

[6] Q. Zhao, P. H. Ni, *Prog. Chem.* **2006**, *18*, 768–779.

[7] A. Roesler, G. W. M. Vandermeulen, H.-A Klok, *Adv. Drug Deliver. Rev*. **2001**, *53*, 95–108.

[8] W. He, T. J. Ding, Z .J. Lu, Q. F. Yang, *Progr. Chem*. **2011**, *23*, 930–940.

[9] A. W. York, S. E. Kirkland, C. L. McCormick, *Adv. Drug Delivery Rev*. **2008**, *60*, 1018–1036.

[10] S. Krishnan, C. J. Weinman, C. K. Ober, *J. Mater. Chem*. **2008**, *18*, 3405–3413.

[11] H. S. Sundaram, Y. Cho, M. D. Dimitriou, C. J. Weinman, J. A. Finlay, G. Cone, M. E. Callow, J. A. Callow, E. J. Kramer, C. K. Ober, *Biofouling* **2011**, *27*, 589–602.

[12] C. S. Gudipati, C. M. Greenleaf, J. A. Johnson, P. Pryoncpan, K. L. Wooley, *J. Polym. Sci. A Polym. Chem.* **2004**, *42*, 6193–6208.

[13] H. Tan, H. Hussain, K. C. Chaw, G. H. Dickinson, C. S. Gudipati, W. R. Birch, S. L. M. Teo, C. He, Y. Liu, T. P. Davis, *Polym. Chem.* **2010**, *1*, 276–279.

[14] M. D. Dimitriou, Z. Zhou, H.-S. Yoo, K. L. Killops, J. A. Finlay, G.Cone, H. S. Sundaram, N. A. Lynd, K. P. Barteau, L. M. Campos, D. A. Fischer, M. E. Callow, J. A. Callow, C. K. Ober, C. J. Hawker, E. J.; Kramer, *Langmuir* **2011**, *27*, 13762–13772.

[15] E. Martinelli, M. K. Sarvothaman, M. Alderighi, G. Galli, E. Mielczarski, J. A. Mielczarski, *J. Polym. Sci. Part A: Polym. Chem*. **2012**, *50*, 2677–2686.

[16] C. Weinman, J. A. Finlay, D. Park, M. Y. Paik, S. Krishnan, H. S. Sundaram, M. Dimitriou, K. E. Sohn, M. E. Callow, J. A. Callow, *Langmuir* **2009**, *25*, 12266–12274.

[17] E. Martinelli, I. Del Moro, G. Galli, M. Barbaglia, C. Bibbiani, E. Mennillo, M. Oliva, C. Pretti, D. Antonioli, M. Laus, *ACS Appl. Mater. Interfaces* **2015**, *7*, 8293–8301.

[18] E. Martinelli, E. Guazzelli, C. Bartoli, M. Gazzarri, F. Chiellini, G. Galli, M. E. Callow, J. A. Callow, J. A. Finlay, S. Hill, *J. Polym. Sci. Part A: Polym. Chem*. **2015**, *53*, 1213–1225.

[19] E. Martinelli, S. Agostini, G. Galli, E. Chiellini, A. Glisenti, M. E. Pettitt, M. E. Callow, J. A. Callow, K. Graf, F. W. Bartels, *Langmuir* **2008**, *24*, 13138–13147.

[20] J. Scheirs (ed.) *Modern Fluoropolymers: High Performance Polymers for Diverse Applications*. John Wiley, New York (**1997**).

[21] Y. Ikada, in *Water in Biomaterials Surface Science*, M. Morra, (ed.), John Wiley, New York, 1st edn, **2001**, p. 291–306.

[22] B. R. Yasani, E. Martinelli, G. Galli, A. Glisenti, S. Mieszkin, M. E. Callow, J. A. Callow, *Biofouling* **2014**, *30*, 387–399.

[23] P. M. Imbesi, N. V. Gohad, M. J. Eller, B. Orihuela, D. Rittschof, E. A. Schweikert, A. S. Mount, K. L. Wooley, *ACS Nano* **2012**, *6*, 1503–1512.

[24] E. Martinelli, G. Galli, S. Krishnan, M. Y. Paik, C. K. Ober, D. A. Fischer, *J. Mater. Chem*. **2011**, *21*, 15357.

[25] D. H. Kaelble, *J. Adhesion* **1970**, *2*, 66–81.

[26] D. K. Owens, R. C. Wendt, *J. Appl. Polym. Sci.* **1969**, *13*, 1741–1747.

[27] D. A. Shirley, *Phys. Rev. B* **1972**, *5*, 4709–4714.

[28] J. F. Moulder, W. F. Stickle, P. E. Sobol, K. D. Bomben, *Handbook of X-ray Photoelectron Spectroscopy*. **1992**. Eden Prairie (MN): Physical Electronics.

[29] N. S. McIntyre, T. C. Chan,in *Practical Surface Analysis 1*, 2nd ed.; D. Briggs, M. P. Seah, (eds.), Wiley: Chichester, U.K., **1990**, p.485–529.

[30] K. Huan, L. Bes, D. M. Haddleton, E. Khoshdel, *J. Polym. Sci., Part A: Polym. Chem.* **2001**, *39*, 1833–1842.

[31] S. Hvilsted, *Polym. Int.* **2014**, *63*, 814–823.

[32] G. Galli, E. Martinelli, E. Chiellini, C. K. Ober, A. Glisenti, *Mol. Cryst., Liq. Cryst*. **2005**, *441*, 211–226.

[33] M. Hikita, K. Tanaka, T. Nakamura, T. Kajiyama, A. Takahara, *Langmuir* **2004**, *20*, 5304–5310.

[34] Y. Y. Durmaz, E. L. Sahkulubey, Y. Yagci, E. Martinelli, G. Galli, *J. Polym. Sci. Part A: Polym. Chem.* **2012**, *50*, 4911–4919.

[35] J. Mielczarski, E. Mielczarski, G. Galli, A. Morelli, E. Martinelli, E. Chiellini, *Langmuir* **2010**, *26*, 2871–2876.

[36] C. Pitois, S. Vukmirovic, A. Hult, D. Wiesmann, M. Robertsson, *Macromolecules* **1999**, *32*, 2903–2909.

[37] L.-T. Weng, K.-M. Ng, Z. L. Cheung, Y. Lei, C.-M. Chan, *Surf. Interface Anal.* **2006**, *38*, 32–43.

[38] E. Martinelli, M. K Sarvothaman, G. Galli, M. E Pettitt, M. E Callow, J. A Callow, S. L. Conlan, A. S. Clare, A. B. Sugiharto, C. Davies, D. Williams, *Biofouling* **2012**, *28*, 571–582.

TABLES

Table 1. Experimental conditions[a)] for the synthesis and physical-chemical properties of block copolymers Si-EFS*x* and Si-FS*y*.

Copolymer	**Si-Br**	**EFS (FS)**	**bipy**	**CuBr**	M_n[b)] **(g mol^{-1})**	M_w/M_n[b)]	M_n[c)] **(g mol^{-1})**	**EFS (FS)[d)] (mol %)**
Si-EFS14	0.26	3.8	0.70	0.28	5300	1.17	5900	81
Si-EFS35	0.13	4.1	0.46	0.15	8300	1.09	13000	91
Si-EFS71	0.07	4.4	0.21	0.08	12300	1.15	25200	96
Si-FS19	0.38	5.7	0.96	0.27	3700	1.17	4900	77
Si-FS39	0.22	6.7	0.42	0.15	5900	1.18	8800	87
Si-FS47	0.12	7.3	0.24	0.08	7500	1.23	10300	89

[a)]Initial feed amounts of reagents in mmol. [b)]By SEC. [c)]By ^{1}H NMR. [d)]Mole percentage in the copolymer.

Table 2. Contact angles and surface free energy of polymer films.

Film	θ_w[a)] **(°)**	θ_h[a)] **(°)**	γ_S[b)] **(mN m^{-1})**	γ_S^{db}[b)] **(mN m^{-1})**	γ_S^{pb}[b)] **(mN m^{-1})**
Si-EFS14	89 ± 1	32 ± 1	27.6	23.6	4.0
Si-EFS35	90 ± 2	32 ± 1	27.3	23.6	3.7
Si-EFS71	89 ± 1	31 ± 1	27.8	23.8	4.0
Si-FS19	103 ± 1	33 ± 1	23.9	23.3	0.6
Si-FS39	100 ± 2	32 ± 1	24.7	23.6	1.1
Si-FS47	99 ± 1	34 ± 1	24.4	23.1	1.3
P(EFS)	95 ± 3	33 ± 1	25.5	23.3	2.2
Si-Br	88 ± 3	~ 0	-	-	-
Si-EFS71_8	109 ± 1	32 ± 1	23.7	23.6	0.1

[a)]Contact angle with water and *n*-hexadecane. [b)]Surface free energy with dispersion and polar components.

Table 3. XPS atomic surface compositions of block copolymer and homopolymer films.

Film	**ϕ (°)**	**C (%)**	**O (%)**	**Si (%)**	**F (%)**
Si-EFS14	70	62	22	12	4
	20	66	19	5	10
	70[a)]	63	22	9	6
	20[a)]	62	20	6	12
	theoretical	64	18	3	15
Si-EFS71	70	61	22	9	8
	20	63	20	3	14
	70[a)]	61	22	10	7
	20[a)]	63	19	4	14
	theoretical	65	17	~1	17
P(EFS)	70	71	23	-	6
	20	66	20	-	14
	70[a)]	71	22	-	7
	20[a)]	66	20	-	14
	theoretical	66	17	-	17
Si-FS19	70	59	16	12	13
	20	60	9	6	25
	theoretical	61	4	4	31
Si-FS47	70	58	18	14	10
	20	61	10	6	23
	theoretical	61	2	2	35
P(FS)	70	70	-	-	29

20	60	-	-	33
theoretical	62	-	-	38

[a)]After immersion in water for 7 days.

GRAPHICAL ABSTRACT

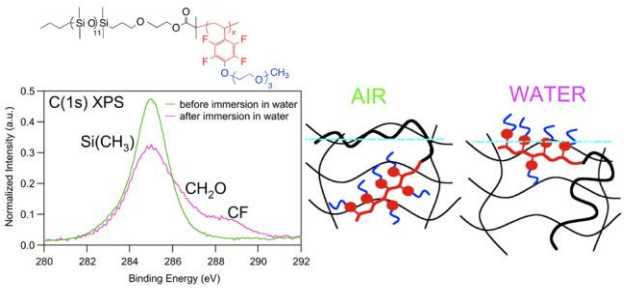

Films of triethylene glycol-modified pentafluorostyrene block copolymers underwent significant surface reconstruction upon immersion in water, resulting in a preferential exposure of the oxyethylenic chains to contact water. Such modification was even more marked when the block copolymer was dispersed in a cross-linked silicone matrix, as the surface concentration of the fluorinated block increased after immersion in water.